Dynamic behaviour of the Allam cycle during load variations with different control strategies

Ilaria Pulvirenti[a], Matteo Pettinari[a], Lorenzo Ferrari[a]

[a] *Department of Energy, Systems, Territory, and Construction Engineering, University of Pisa, Pisa, Italy, i.pulvirenti@studenti.unipi.it, matteo.pettinari@phd.unipi.it, lorenzo.ferrari@unipi.it* ***(CA)***

Abstract:

To mitigate climate change, developing technologies capable of reducing pollutant emissions is crucial. Although carbon capture has been widely studied, costs remain higher than expected, while fossil fuels continue to dominate global power generation. This context highlights the need for power cycles able to use hydrocarbon fuels while avoiding CO_2 emissions.

The Allam cycle is an oxy-combustion, semi-closed, supercritical CO_2 power cycle that inherently captures carbon dioxide while operating with methane or solid fuels. Its combustion process produces only water and CO_2, the latter serving as the working fluid, part of which is extracted at high pressure for transport and storage. Despite numerous studies in the literature focusing on the Allam Cycle, comprehensive analyses of its transient behaviour are still limited, yet understanding its dynamic response is essential for assessing real-world operability and for guiding the design of components and control systems that can safely operate the system at part-load.

This article presents a simplified dynamic model of the Allam cycle, which was utilised to investigate its dynamic behaviour under load variations with different control strategies. Results show that the temperature-based load control strategy provides the fastest and most accurate tracking of load changes compared to the inventory control, thereby appearing much better suited for applications requiring rapid load modulation. Conversely, the inventory control approach better preserves system performance in off-design conditions, with response time strongly dependent on system volume.

Keywords:

Allam cycle; Dynamic analysis; Load variation; Operability; Supercritical CO_2.

1. Introduction

1.1. State of the art and literature review

The main oxy-fuel combustion power cycles include the Semiclosed Oxycombustion Combined Cycle (SCOC-CC), Allam, Graz, and Clean Energy Systems (CES) cycles [1]. All use pure oxygen to burn fuel, capture nearly all CO_2, and recover heat through turbines and heat exchangers, though their configurations differ.

Comparative studies [2] show that the Allam cycle achieves the highest efficiency (~55 %) and the lowest levelised cost of electricity (~84 €/MWh), making it the most promising oxy-combustion technology for low-emission, cost-effective power generation.

The Allam cycle is a high-pressure, highly recuperated Brayton cycle using a trans-critical CO_2 working fluid [3,4]. Its process diagram is illustrated in Figure 1. Fuelled by natural gas or solid fuels that undergo gasification, it operates with pure oxygen supplied by an Air Separation Unit (ASU) and a high-pressure CO_2 stream that acts as a diluent to moderate combustion temperature. Methane combusts with oxygen, producing CO_2 and H_2O [5]. The hot exhaust expands through a turbine (points 1-2), generating power, and then passes through a recuperative heat exchanger (pt. 2-3) to preheat the incoming CO_2 recycle stream. Water condenses (pt. 4-5) and is separated, while most CO_2 is recycled, with nearly 5 % extracted to maintain mass balance in the cycle, as a high-purity stream for sequestration or use. Compression is achieved in a multi-stage CO_2 compression train with intercooling, raising the working fluid pressure from 30 to 300 bar (pt. 5-6).

Additional heat input can be sourced from the waste heat generated by the air compressors of the ASU, thereby reducing the fuel energy input required for the combustor. As such, the Allam cycle combines high-

pressure CO_2 recirculation, recuperation, and selective heat addition to achieve high efficiency, inherent CO_2 capture, and reduced fuel consumption [6].

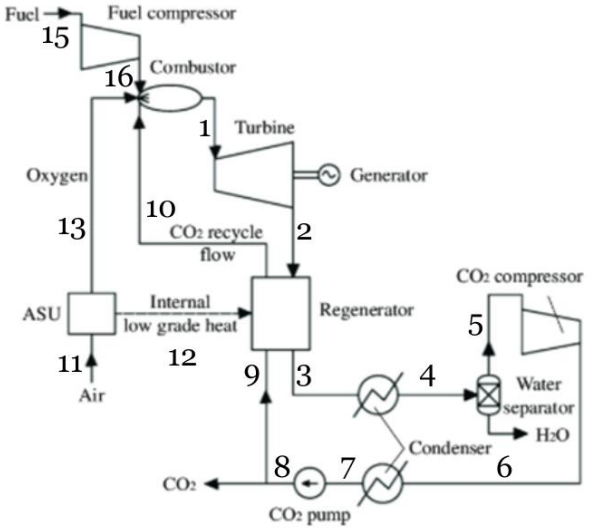

Figure. 1. Process diagram of natural-gas-fuelled Allam cycle [7].

Given the novelty and potential of the Allam cycle, academic researchers began focusing their attention on this promising and zero-emission solution for producing energy from fossil fuels. Numerous studies have been conducted since 2011, when the Allam cycle was first presented to the public. In 2016, the first systematic optimisation of the cycle's efficiency was conducted, along with a sensitivity analysis on the influence of different variables on the cycle's performance [8]. It was found that the net plant electric efficiency is equal to 54.8 % with 100 % CO_2 capture.
In 2020, a modified Allam cycle with recompression was proposed [9], where part of the recirculated CO_2 is extracted after the condenser, compressed, and used both as a cooling flow and to bridge the heat gap between low- and high-pressure CO_2 streams in the regenerator, eliminating the need for additional heat from the ASU. The study reports an efficiency of 49.34% without ASU heat integration, which increases to 52.88% with recompression. A novel layout of the Allam cycle, which combines a reheating configuration with the original Allam cycle, was also investigated [10]. The net efficiency of the optimised Allam cycle with reheat is up to 49.32 %, slightly higher than that of other oxy-combustion cycles and about 5 % lower than that of the original Allam cycle. However, it shows a power production increase of 2.1–2.2 times that of the original Allam cycle. A study conducted in 2025 [11] showed that the Allam cycle achieves efficiencies of about 51 %, with performance mainly affected by the regenerator design: an optimal UA range of 30.000 – 43.000 kW/K was identified as a good compromise between efficiency and heat exchanger size. CO_2 compression and pumping were identified as the main areas for improvement, supporting future techno-economic optimisation.

1.2. Paper contributions

While most research focuses on cycle optimisation, the dynamic modelling and subsequent transient analysis of the Allam cycle have received little attention in the open literature, despite being fundamental for understanding its real-world operation. In fact, analysing the system's dynamic behaviour is essential not only to gain insight into its transient characteristics and overall stability, but also to support the design and optimisation of its components, to evaluate its capability to provide grid services, and to identify potential operational limitations.
Given such a knowledge gap, the present work focuses on investigating the dynamic response of the Allam cycle under various operational scenarios. Specifically, after developing a dynamic model of the system capable of capturing its relevant dynamics and implementing different control strategies to operate the system, the study examines how the cycle behaves under load variations with different control strategies, which are:

- Temperature-based load control strategy;
- Inventory load control strategy.

A comparative analysis is further provided to highlight the performance and limitations of the two approaches. Ultimately, the impact of the system volumes is investigated throughout an extensive sensitivity analysis.

2. Methodology

2.1. Component modelling

The Allam cycle dynamic model was developed in MATLAB® R2023a (The MathWorks Inc., 2023) using Simscape™. CoolProp was used within the MATLAB® environment to compute the thermodynamic and physical properties of CO_2. Some assumptions and simplifications were made due to limited information on some plant components and the ease of the modelling process. Notably, the circulating fluid and fuel were assumed to be pure CO_2, as well as the fluid exiting the combustion chamber (water and other gases were not considered). This assumption is supported by the fact that the mixture exiting the turbine consists of more than 90% carbon dioxide [3]. Turbomachinery was considered to operate at a fixed physical rotational speed. The secondary side (water side) of the coolers and of the heater connected with the ASU was not modelled explicitly but instead idealised as a controlled thermal power source. The thermal inertia of the components was also neglected, since the analyses were performed assuming the system to be already at design temperature. The cycle components were modelled following [4], ensuring consistency with the literature and a validated modelling framework. Figure 2 illustrates the components included in the Allam cycle model.

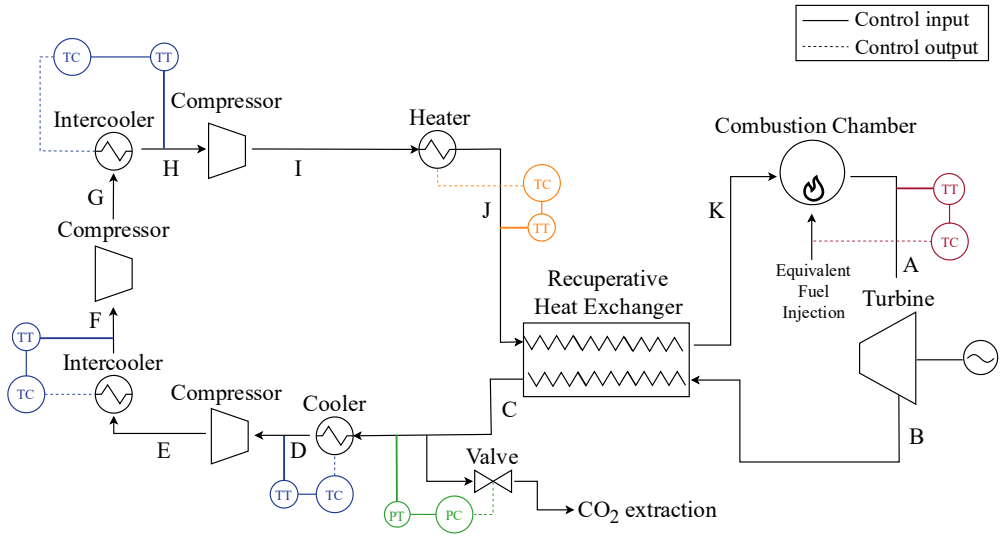

(a)

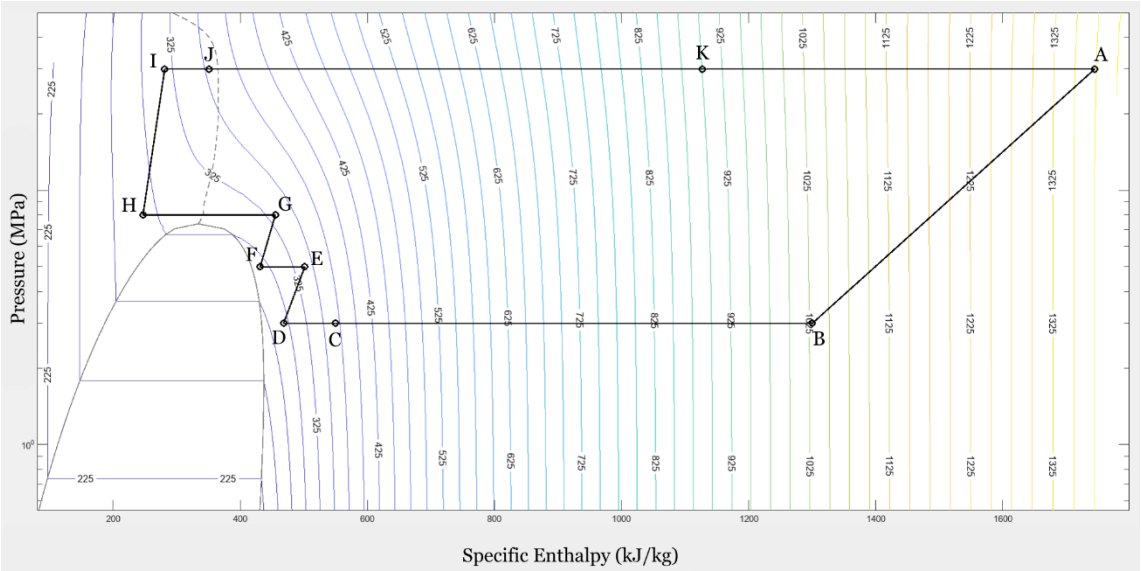

(b)

Figure. 2. (a) Simplified schematic of the Allam cycle modelled in Simscape™ with temperature and pressure control systems. Blue loops refer to the compressor inlet temperature controls. The green loop entails the extraction valve controller, whilst the orange and red loops indicate the ASU heater and combustion chamber controls, respectively; (b) *p-h* diagram.

Turbomachinery. Due to the limitations of the built-in Simscape™ compressor and turbine components, a custom lumped-parameter block for turbomachinery was developed. Notably, compressor maps were obtained by scaling those available in [6], while turbine maps were scaled from [12] to match the characteristics of the analysed system. The model neglects the thermal inertia and internal gas volume of the machines, as these are typically negligible compared to the thermal masses and volumes of the heat exchangers and piping. Shaft dynamics are not included, as turbomachinery is assumed to operate at a fixed rotational speed. Ventilation effects, back-flow phenomena, and other complex fluid-dynamic behaviours near stall are not explicitly represented, while simplified assumptions are made for what concerns the behaviour in surge or choked regions. The model reproduces both design and off-design operation by relying on performance maps.

Heat exchangers and combustion chamber. The three coolers, the heater connected with the ASU, the recuperative heat exchanger and the combustion chamber were modelled by adopting a high-level approach, since detailed information concerning the design of such components is currently not available in the literature. The block utilised captures mass and energy storage of a fixed fluid volume exchanging heat with a thermal network, under lumped-parameter (0D) assumptions and neglecting gravity, thermal resistance, and flow losses. Notably, only the gas side of the coolers was explicitly represented and modelled as lumped (0D) constant volume chambers, whose flows abide energy, mass and momentum balances. Conversely, the water side was idealised as a controlled thermal power source, effectively mimicking a secondary cooling circuit that maintains a prescribed inlet temperature. Thermal inertia was not included as the system components are assumed to be already at design temperature.
The same modelling approach was applied to the heater receiving heat from the ASU. Conversely, the recuperative heat exchanger——being more complex and poorly documented in the literature——was discretised into seven chambers on both the hot side and cold side, connected through thermal resistive elements, thereby approximating a 1D component capable of capturing the temperature profiles evolving within the heat exchanger. The thermal resistance of the recuperator was derived using the ε–NTU method, assuming a counterflow arrangement and constant convective heat transfer coefficients; an overall thermal resistance of approximately 10^{-8} K/W was then obtained. The same approach was also used to determine the overall heat transfer area and gas volume of all the heat exchangers. A compactness factor of 500 m^2/m^3 was assumed to estimate the coolers and recuperator volumes, consistent with values for moderately compact heat exchangers. The heater connected with the ASU was excluded from this sizing procedure due to limited available data.
Regarding the combustion chamber, the heat released to the working fluid from the combustion reaction is controlled through a dedicated control system. Pure methane is assumed as the fuel, and its reaction with oxygen is simplified to produce only CO_2. The introduction of this CO_2 into the cycle is represented by a controlled mass flow source, which injects the exhaust flow at the outlet pressure and temperature of the chamber without additional losses. For clarity and brevity, the detailed equations characterising Simscape™ blocks are not included and can be found in The MathWorks Inc. (2006).

Extraction valve. To maintain the minimum cycle pressure at 30 bar while keeping the system inventory constant, the CO_2 entering through combustion must be extracted. For this purpose, an extraction valve was implemented downstream of the recuperative heat exchanger and modelled as an adiabatic variable size orifice. The valve was sized to discharge 50 kg/s under a 10 bar pressure differential at full opening, and its position is regulated by a dedicated control system. The extracted CO_2 is assumed to be stored in an idealised 20 bar environment.

2.2. Control systems

Several control systems, outlined in Figure 2, were implemented to ensure that the model of the Allam cycle operates toward the desired operating conditions.

Compressors' inlet temperature control. The inlet temperature of the three compressors is maintained at 293.15 K through independent PI feedback controllers, each adjusting the cooling power of the corresponding cooler based on the downstream compressor inlet temperature residual. The coolers' actuation dynamics are represented by a first-order transfer function with a time constant of 2 s, modelling the response time of the water feed system at the secondary end of the cooler, and allowing for a more realistic prediction of transient behaviour. Saturation limits of the control action are also considered, ensuring a physically consistent cooling behaviour; as such, a back-calculation scheme is adopted to prevent integrator windup. Lastly, as for the other controls detailed in the following, gains were determined through trial-and-error.

ASU control. Downstream of the compression train, the heat exchanger recovering excess heat from the ASU is also regulated by a PI feedback controller. Due to limited information on the ASU's integration with the Allam cycle, the outlet temperature setpoint is fixed at 353.15 K, independently of the variable heat available from oxygen production. Any surplus heat that would raise the fluid above this value is conceptually dissipated by an auxiliary component not included in the model. The controller output defines the thermal power transferred to the working fluid, with a lower saturation limit preventing non-physical negative values. The back-calculation anti-windup strategy is again applied to ensure stable behaviour under saturation. Actuation dynamics for this exchanger are neglected due to insufficient data, and their influence on the overall system response is assumed to be minimal.

Turbine inlet temperature control. The turbine inlet temperature is controlled through a dedicated PI feedback system, with a setpoint of 1373.15 K. Based on the temperature residual, the controller modulates the thermal power delivered by the combustion chamber, subject to lower and upper saturation limits to prevent unrealistic cooling or excessive fuel supply. Because the combustion chamber may reach its physical limits during operation, an anti-windup mechanism is implemented to avoid integrator windup. From the controller output (e.g., the thermal power delivered by the combustion chamber), the required fuel flow and the resulting CO_2 production are computed assuming stoichiometric oxy-combustion, making them directly proportional to the demanded thermal power. The combustion dynamics are represented by a first-order system with a 0.5 s time constant, ensuring rapid adjustment of both heat release and CO_2 injection into the cycle.

Extraction valve control. A PI feedback controller is used to regulate the CO_2 extraction valve in order to maintain the minimum cycle pressure at 30 bar. The valve operates only in the discharge direction: it opens when the pressure exceeds the setpoint and remains closed when the pressure falls below it. When the pressure decreases, the model includes no pumps to inject additional fluid from an external reservoir, so any increase in the internal mass inventory comes solely from the CO_2 added through combustion. The controller output, bounded between 0 (fully closed) and 1 (fully open), determines the normalised valve stroke. Because the controller operates under saturation, a back calculation anti-windup scheme is applied to ensure stable behaviour. The valve actuation dynamics are modelled as a first-order system with a time constant of 1 s, meaning that, under a 10-bar pressure drop, it reaches 99.3 % of the nominal 50 kg/s discharge capacity in approximately 5 s.

Load controls. Two load control strategies were designed to vary the total power output of the system.

1. The temperature-based strategy relies on two separate control loops. The first loop consists of a cascade PI control demanded to regulate the system's power output. Notably, the outer controller determines the target turbine inlet temperature to achieve the desired power output. The inner controller then regulates the thermal power released by the combustion chamber based on the turbine inlet temperature residual and, consequently, determines the CO_2 injected into the cycle after combustion. Conversely, the second control scheme is a simple PI feedback controller that adjusts the extraction valve opening to maintain the minimum cycle pressure at 30 bar.

2. The inventory strategy relies on two PI feedback loops. The first regulates the extraction valve opening to reach the desired power level, while the second maintains the combustion chamber outlet temperature—hence, the turbine inlet temperature—at 1373.15 K, thus determining the thermal power to be released and the associated CO_2 production.

2.3. Steady-state analysis and investigated scenarios

After assembling the Simscape™ model of the Allam cycle and implementing the related control strategies, the system was simulated to determine its steady-state conditions under the design assumptions. The resulting thermodynamic properties and component power levels define the reference design point, detailed in Table 1. In particular, when operating at design conditions, the system delivers a total output power of 331.08 MW, with an overall efficiency of 59.59 %. The CO_2 inlet mass flow rate, which at steady state is equal to the outlet mass flow rate, is 30.48 kg/s.

To assess the dynamic behaviour of the Allam cycle and evaluate its performance and efficiency under load variations, the system response to a ±10% change in net power, applied at a rate of 2.5 MW/s, was studied using the two load control strategies previously described. A sensitivity analysis on the heat exchangers' volume was further performed to evaluate its effect on the system's transient behaviour. Specifically, the configurations examined include a scenario in which all the heat exchangers have a volume of 1 m^3, a scenario where they have half of the design volume, and a scenario where they have the design volume, obtained throughout the theoretical sizing of the component previously described. These analyses provide insight into the Allam cycle's dynamic response, operational flexibility, and control requirements under realistic transient conditions

Table 1. Thermodynamic properties (pressure and temperature) and mass flow rates at the design point of the Allam cycle model. LP, IP and HP stand for Low-, Intermediate-, and High-Pressure, respectively.

Points	Description	Pressure [bar]	Temperature [K]	Mass flow rate [kg/s]
A	Turbine Inlet	299.83	1373.15	929.48
B	Turbine Outlet	30.00	1028.95	929.48
C	LP Cooler Inlet	30.00	368.12	899.01
D	LP Compressor Inlet	30.00	293.15	899.01
E	LP Compressor Outlet	49.99	432.15	899.01
F	IP Compressor Inlet	49.99	293.15	899.01
G	IP Compressor Outlet	79.98	331.94	899.01
H	HP Compressor Inlet	79.98	293.15	899.01
I	HP Compressor Outlet	299.83	318.74	899.01
J	Recuperative Heat Exchanger Inlet	299.83	353.15	899.01
K	Combustor Inlet	299.83	900.26	899.01

3. Results

The system is operated at nominal power from 0 s to 1120 s and from 3914 s to 6000 s; between 1120 s and 1134 s, a 10 % downward load ramp is imposed, after which the system operates at the reduced load from 1134 s to 3900 s. Finally, between 3900 s and 3914 s, a 10 % upward ramp is applied, restoring the system to its nominal operating point.

3.1. Temperature-based load control

Figure 3a shows how the cycle's power output follows the setpoint profile. The temperature-based strategy enables the cycle to follow the power setpoint almost perfectly, responding quickly to both decreases and increases in power output.

Figure 3b shows how the cycle's efficiency varies due to load changes. It is noteworthy that the system exhibits an inverse response: when the downward load ramp is imposed at 1120 s, the efficiency initially tends to increase, but later it settles at a lower value than the nominal one. The opposite behaviour can be observed when the upward load ramp is applied at 3900s. The same inverse response can also be observed in the extraction valve opening in Figure 3c.

The inverse response can be explained by the transient variations of the thermodynamic properties and mass flow at the compressors and turbine inlets (Figures 3d, 3e, 3f). Notably, when the power output setpoint is reduced, the turbine inlet temperature undergoes a fast and significant drop of more than 200 K due to the temperature-based load control, while the compressors' inlet temperatures remain fixed at the 293.15 K setpoint, thanks to the control loops implemented on the coolers. When the fluid entering the turbine becomes colder, its density increases, which in turn leads to a higher actual mass flow rate through the turbine. However, because the colder fluid also has a lower enthalpy, the turbine has less thermal energy available to convert into mechanical work. As a consequence, even with the increased mass flow rate, the turbine delivers less power. This reduction in released expansion energy also results in a smaller pressure drop across the turbine. Since the turbine processes a higher actual mass flow rate, its instantaneous efficiency temporarily increases due to this dynamic effect (Figure 3b). Nonetheless, the reduction in pressure ratio causes the maximum cycle pressure to decrease and the minimum pressure to increase. As a result, the extraction valve opens in order to remove mass and restore the minimum cycle pressure to 30 bar.

At steady state, after the downward load ramp, the turbine inlet temperature is lower, which leads to a reduction in the useful power output. However, its efficiency becomes higher than in the nominal scenario (Figure 3b) because the turbine processes a larger actual mass flow rate. This increase in mass flow rate at steady state occurs because the lower fluid temperature increases its density, allowing more fluid to flow through the turbine and the compressors compared to the nominal case.

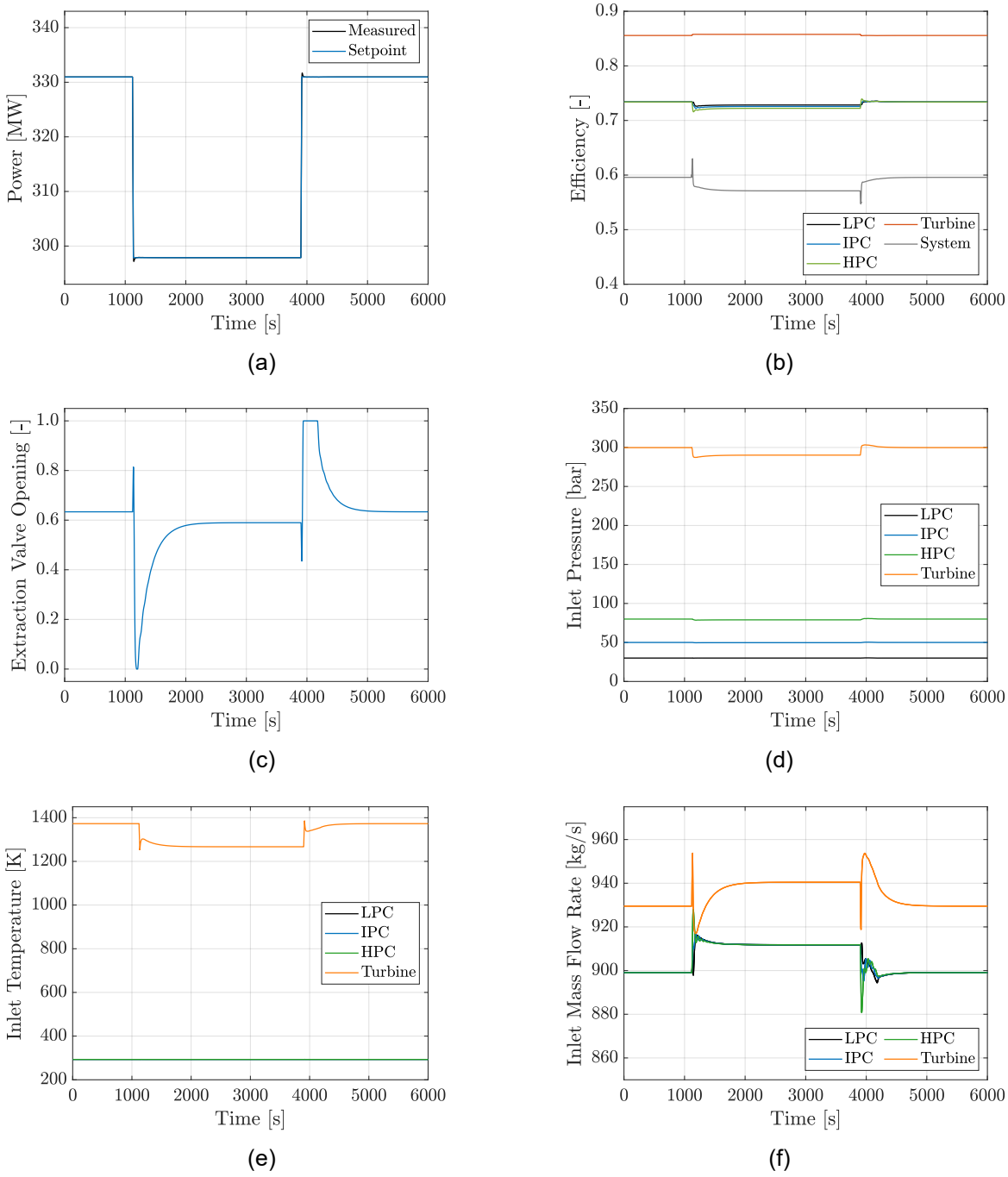

Figure. 3. Dynamic response of the Allam cycle during 10 % load variations under the temperature-based load control strategy: (a) Comparison between imposed and actual power; (b) Turbomachinery and system efficiency evolution; (c) Extraction valve normalised opening; (d) Turbomachinery inlet pressure; (e) Turbomachinery inlet temperature; (f) Turbomachinery inlet mass flow rate.

3.2. Inventory load control

Figure 4a illustrates the system's response, showing how the cycle's actual load tracks the imposed setpoint throughout the simulation. It can be noted that, with this load control strategy, the system responds significantly slower to load changes compared to the temperature-based strategy. The settling time for the downward ramp is approximately 900 s, while for the upward ramp it is around 575 s.

This difference in the system's response time is primarily due to the plant's intrinsic design features; notably, during a power reduction, the valve takes longer to adjust to the lower flow requirements, since it is already fully open and cannot release additional flow more rapidly, thereby resulting in a slower system response. As the valve is fully open, the power load decreases almost linearly, with a rate closely related to the valve's characteristics and the volume of the fluid to be discharged. Faster response times could then be achieved by improving the extraction valve system. Conversely, when the load increases, the valve can reduce

its opening, allowing additional CO_2 to remain within the cycle (Figure 4c) and thus leading to a faster system response. Although the extraction valve is fully closed, the gradual increase in system mass depends on the rate at which the cycle volume is replenished, which is governed by the combustion chamber control. This highlights that the slow response during load increase is primarily dictated by the very large system volume.

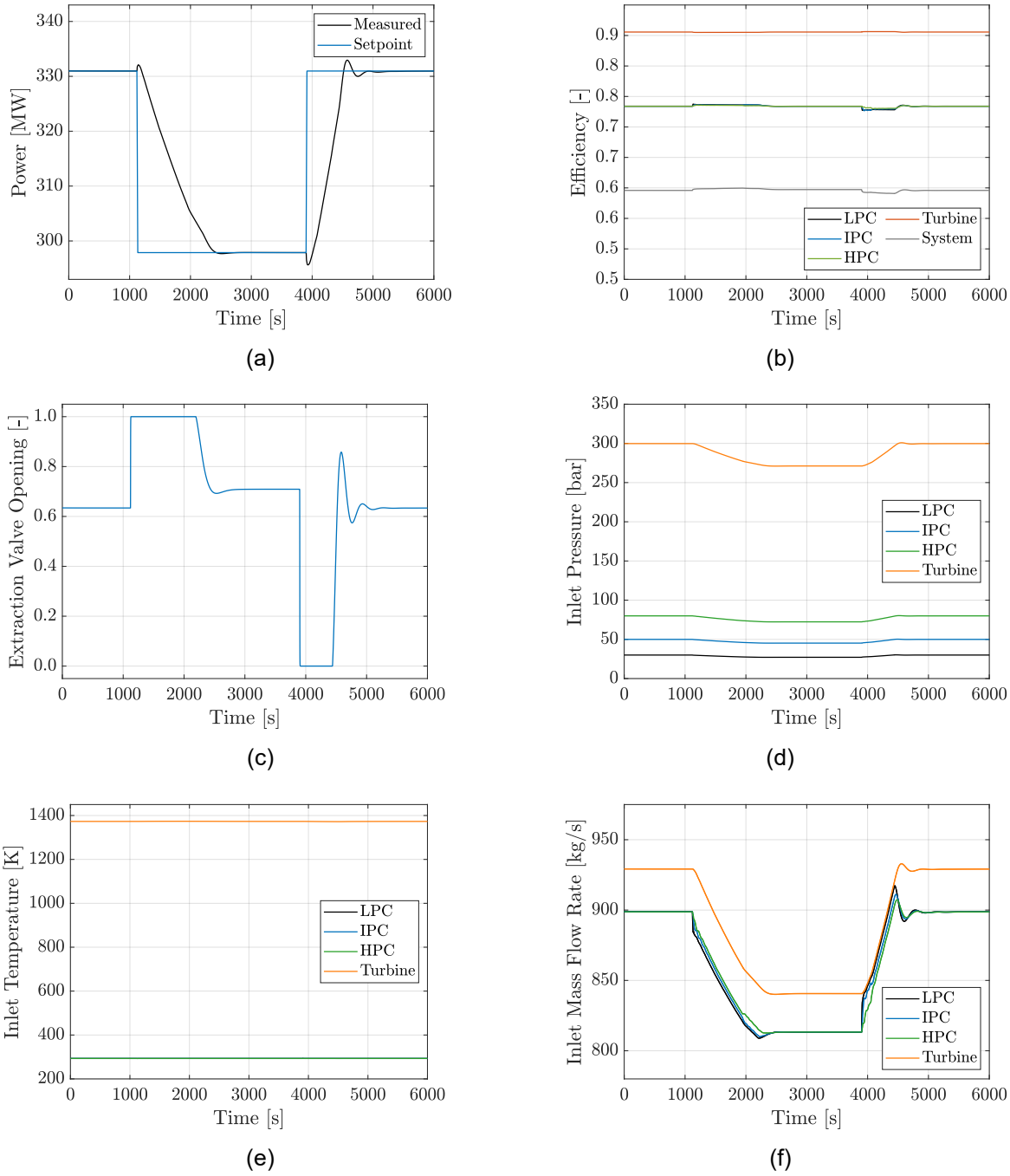

Figure. 4. Dynamic response of the Allam cycle during 10 % load variations under the inventory load control strategy: (a) Comparison between imposed and actual power; (b) Turbomachinery and system efficiency evolution; (c) Extraction valve opening; (d) Turbomachinery inlet pressure; (e) Turbomachinery inlet temperature; (f) Turbomachinery inlet mass flow rate.

In order to follow the power setpoint during the descending ramp, the cycle behaves as a second-order system, exhibiting an initial overshoot of approximately 1 MW (Figure 4a). A similar behaviour is observed during the upward ramp, but in the opposite direction. Specifically, when the downward ramp is imposed, the cycle power output initially increases. This occurs because, in order to reduce the power, the extraction valve opens fully to release mass flow; however, despite being fully open, it cannot extract the required mass flow quickly enough to match the desired reduction in total power, resulting in the initial overshoot. Once the desired mass flow is extracted and a new equilibrium is reached, the valve partially closes, while the system continues to follow the power setpoint. The system efficiency is not

significantly influenced by the load ramp variations, as shown in Figure 4b.
In this second scenario, the inlet temperatures of the turbine and the compressors are maintained at constant values by their respective control loops, and to achieve a reduction in the produced power, the system decreases its overall working fluid mass flow rate. This reduction is illustrated in Figure 4f. As shown in Figure 4d, the pressure ratio across the turbine also decreases in order to reduce the useful power produced by the turbine, and consequently, the total cycle power output. This effect is particularly evident on the maximum cycle pressure. Overall, the system effectively adjusts its internal energy flows to accommodate changes in power demand, without introducing significant efficiency losses or instability in the thermodynamic process.

3.3. Comparative analysis of the load control strategies

As can be observed in Figure 5a, the temperature-based load control allows the system to follow the setpoint almost perfectly, exhibiting a fast response both during decreases and increases in power output. In contrast, the inventory load control strategy leads to a considerably longer response time for the same power changes. This difference highlights that the temperature-based approach is more suitable for applications where the Allam cycle power plant is required to adjust its output quickly to regulate the grid and provide ancillary services, which can be economically valuable. However, achieving such high responsiveness comes at a cost: the turbomachinery must undergo larger operating changes to track the setpoint, which leads to a greater impact on both components' and overall cycle efficiency (Figure 5b).
Overall, this analysis highlights that the temperature-based strategy prioritises fast, accurate tracking and system flexibility, while the inventory strategy presents a more conservative operation and reduces the impact on cycle efficiency, partly due to smaller disturbances in the operating points of the turbomachinery (Figures 5c, 5d, 5e, 5f). The fast response provided by the temperature-based strategy makes it particularly suitable for applications requiring rapid adjustments, such as grid regulation and the provision of ancillary services. Therefore, the choice between the two strategies depends on whether rapid response or minimal impact on overall system efficiency is the primary design objective.

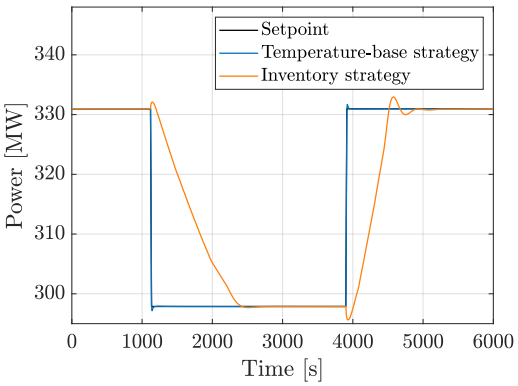

(a)

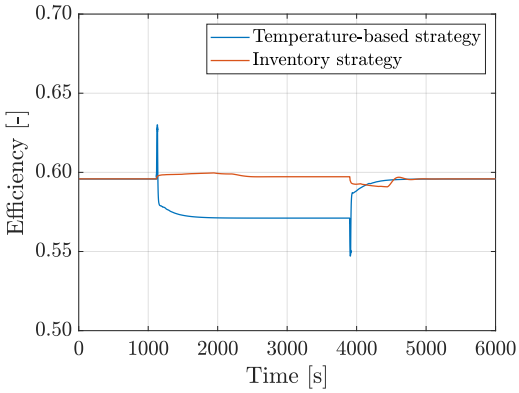

(b)

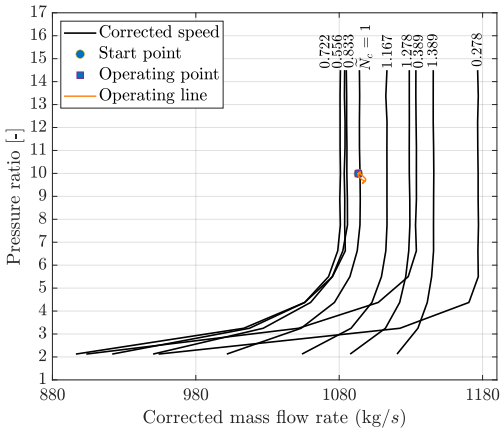

(c)

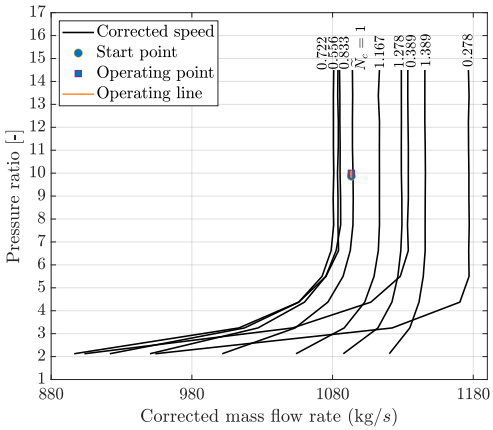

(d)

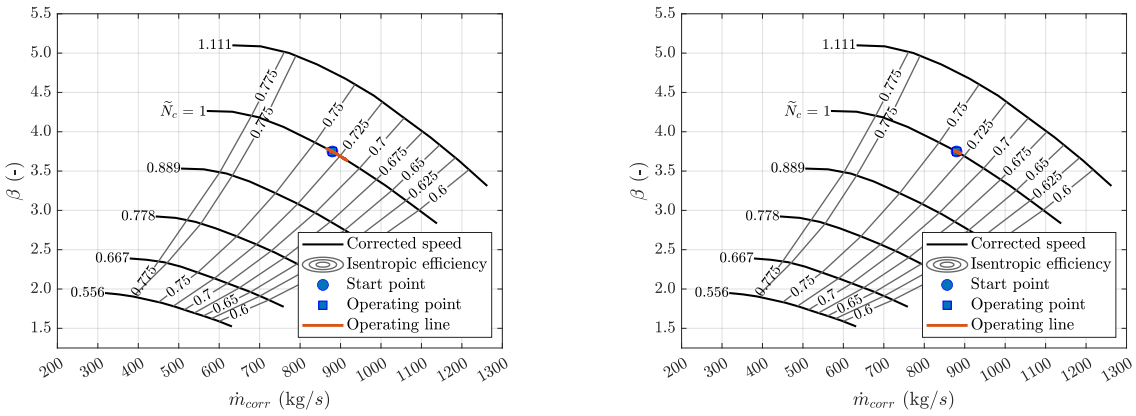

(e) (f)

Figure. 5. Comparison of the dynamic response of the Allam cycle while operated with the two load control strategies: (a) Imposed and actual power output; (b) System efficiency evolution; (c) Turbine operating point evolution under the temperature-based load control strategy; (d) Turbine operating point evolution under the inventory load control strategy; (e) HP Compressor operating point evolution under the temperature-based load control strategy; (f) HP Compressor operating point evolution under the inventory load control strategy.

3.4. Sensitivity Analysis for Different System Volumes

In order to evaluate how the system volume influences the effectiveness of the two load control strategies, a sensitivity analysis was carried out. The objective was to investigate how the system dynamics, performance, and ability to track the imposed power setpoint vary when its overall volume is modified (e.g., heat exchangers, piping, etc.). In particular, the study aims to determine the impact of system volume on transient behaviour during load changes, including the response speed, the magnitude of oscillations, and the overall accuracy in tracking the desired power output, thereby providing a more complete understanding of the operability of the Allam cycle under realistic variations in system hardware. Three configurations were examined. The first represents a unit-volume system, in which all heat exchangers were assigned a volume of 1 m^3. The second configuration corresponds to a half-design-volume system, where the three coolers and the recuperative heat exchanger were assigned half of their nominal design volumes. These two cases were then compared with the previously analysed system operating with its original design volumes. It is important to highlight that the volume of the heat exchanger connected to the ASU was not included in this parametric investigation and was instead kept fixed at 1 m^3. This choice is justified by the lack of reliable data in the literature regarding its actual characteristics, which makes any hypothetical scaling questionable.

Figure 6 depicts the main differences occurring in the system evolution due to volume variation. Notably, Figures 6a and 6b illustrate that, while the system's response time under the temperature-based approach is unaffected, under the inventory control a smaller system volume led to a faster response and quicker convergence to the setpoint power, whereas larger volumes produced slower, smoother dynamics. The unit-volume configuration exhibited sharper oscillations and more abrupt variations, as can be observed in the behaviour of extraction valve opening in Figure 6d, highlighting a trade-off between response speed and mechanical stability.

Figure 6c shows that with the temperature-based control strategy the inverse response of the extraction valve disappeared in the unit-volume configuration, and the cycle reached steady state more quickly. This behaviour is due to the rapid thermodynamic response of the unit-volume system. During the downward load ramp, the turbine inlet temperature drops almost immediately, causing the much smaller amount of working fluid to cool and become denser. As a result, both the maximum and minimum cycle pressures drop sharply, prompting the extraction valve to close to restore the minimum pressure setpoint of 30 bar. This mechanism differs from that of the half-design- and design-volume systems, where the larger fluid inventory in the heat exchangers dampens the immediate effect of the temperature drop, leading to a temporary rise in minimum pressure and an initial valve opening before the system reaches the new equilibrium.

Overall, reducing system volume accelerates the transient response for both control strategies but has a different effect on oscillations: while for the temperature-based control strategy larger volumes imply bigger and more prolonged oscillations, for the inventory control strategy they produced slower, smoother dynamics with reduced mechanical stress.

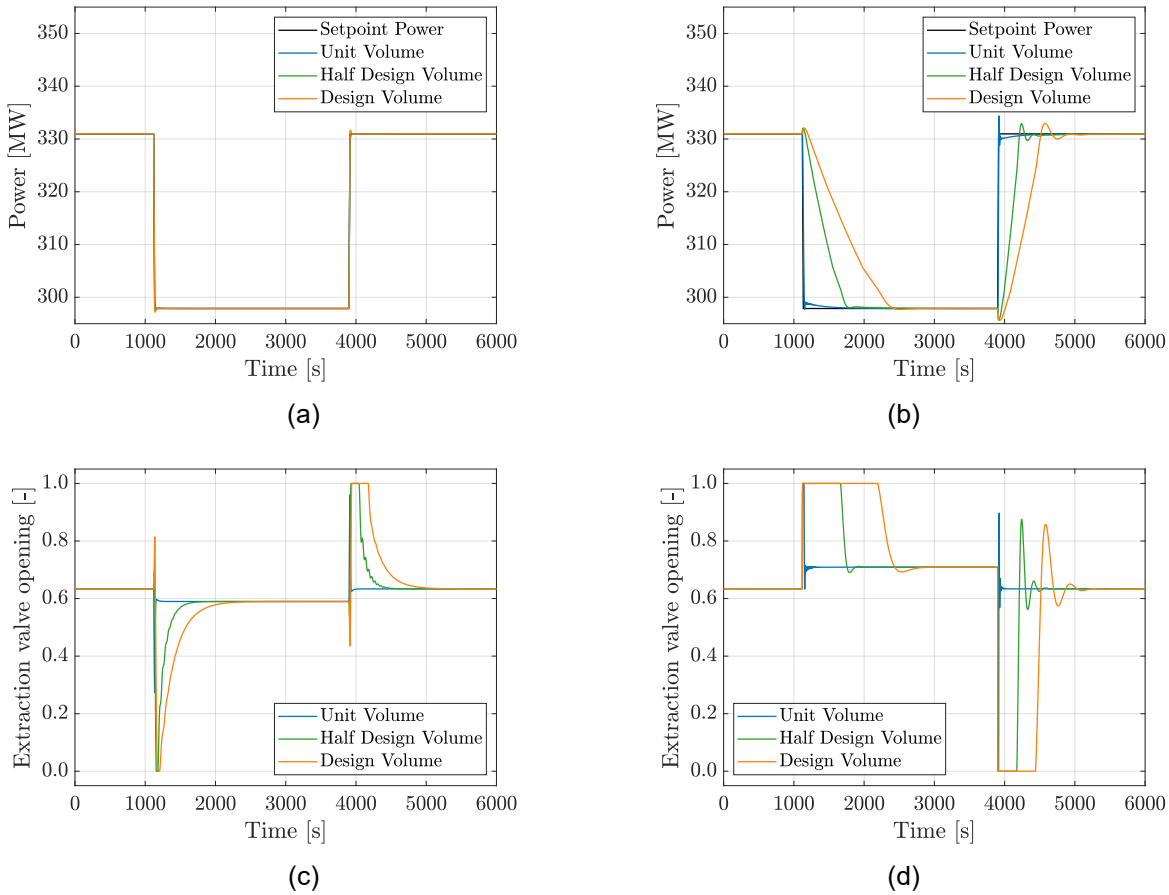

Figure. 6. Effect of different system volume: (a) System power output evolution under the temperature-based load control strategy; (b) System power output evolution under the inventory load control strategy; (c) Extraction valve opening under the temperature-based load control strategy; (d) Extraction valve opening under the inventory load control strategy.

4. Conclusions

The Allam cycle is a promising technology for net-zero-emission power generation using hydrocarbon fuels. While its design has been widely studied, its dynamic behaviour has received little attention so far, even though understanding transients is crucial for assessing operability, components design and selection, grid support, and commercial readiness.

Within the present study, a dynamic model of the Allam cycle was developed and subsequently utilised to evaluate the cycle performance under load variations imposed through a downward ramp corresponding to 10 % of the nominal power, followed by an upward ramp that restored the system to its rated operating point. Two load control strategies were analysed. Notably, the temperature-based strategy, regulating turbine inlet temperature, allows the system to track the power setpoints quickly and accurately, while the inventory strategy, controlling the cycle CO_2 inventory throughout the extraction valve, responds more slowly. Therefore, the first strategy appears better suited for applications requiring rapid load modulation, such as grid stabilisation or the provision of ancillary services. System volume, mainly determined by the heat exchangers, was found to strongly influence the cycle dynamic response; in particular, for the temperature-based strategy, reducing the volume eliminates the inverse response observed in the nominal system configuration, although it does not significantly alter the overall response time. For the inventory control strategy, however, a unit-volume system—i.e. a substantially reduced fluid inventory—achieves remarkably accurate setpoint tracking, outperforming both the half-design and design-volume configurations. In general, reducing the system volume results in faster dynamic responses and quicker convergence to a new steady state. However, in the inventory control strategy, this comes at the expense of increased oscillations and sharper transients, which may raise mechanical and thermal stresses on components. These findings highlight the need to carefully balance dynamic responsiveness and component durability when designing or scaling the Allam cycle for practical operation.

Future research may focus on improving the dynamic modelling of key components, particularly heat exchangers, and on implementing advanced control strategies to enhance system response under load variations.

Nomenclature

Acronyms

ASU	Air Separation Unit
HPC	High-Pressure Compressor
IPC	Intermediate-Pressure Compressor
LPC	Low-Pressure Compressor
PC	Pressure Control
PI	Proportional-Integral control
PT	Pressure Transducer
TC	Temperature Control
TT	Temperature Transducer

References

[1] Darabkhani, H., Varasteh, H., Bazooyar, B. (2023). Oxyturbine power cycles and gas-CCS technologies. In: Carbon Capture Technologies for Gas-Turbine-Based Power Plants (pp. 39-74). Elsevier.

[2] Mancuso, L., Ferrari, N., Chiesa, L., Martelli, E. Romano, M. (2015). Oxy-combustion turbine power plants. Technical report, Amec Foster Wheeler Italiana and Politecnico di Milano.

[3] Allam, R. J., Fetvedt, J. E., Forrest, B. A., Freed, D. A. (2014). The oxy-fuel, supercritical CO_2 Allam cycle: new cycle developments to produce even lower-cost electricity from fossil fuels without atmospheric emissions. Proceedings of ASME Turbo Expo 2014: Turbine Technical Conference and Exposition, vol. 3B: Oil and Gas Applications; Organic Rankine Cycle Power Systems; Supercritical CO_2 Power Cycles; Wind Energy, Düsseldorf, Germany.

[4] Allam, R. J., Martin, S., Forrest, B., Fetvedt, J., Lu, X., Freed, D., Brown Jr., G. W., Sasaki, T., Itoh, M., Manning, J. (2017). Demonstration of the Allam cycle: an update on the development status of a high efficiency supercritical carbon dioxide power process employing full carbon capture. Energy Procedia, 114, 5948 – 5966.

[5] Sleiti, A. K., Al-Ammari, W. A. (2021). Energy and exergy analyses of novel supercritical CO_2 Brayton cycles driven by direct oxy-fuel combustor. Fuel, vol. 294, 120577.

[6] Jiang, P., Wang, B., Tian, Y., Xu, X., Zhao, L. (2021). Design of a supercritical CO_2 compressor for use in a 1 MWe power cycle. ACS Omega, 6(49):33769–33778.

[7] Rogalev, A. N., Rogalev, N. D., Kindra, V. O., Grigoriev, E. Y., Makhmutov, B. A. (2019). The flow path characteristics analysis for supercritical carbon dioxide gas turbines. E3S Web of Conferences, vol. 124:01006.

[8] Scaccabarozzi, R., Gatti, M., Martelli, E. (2016). Thermodynamic analysis and numerical optimization of the NET Power oxy-combustion cycle. Applied Energy, 178:505–526.

[9] Zhang, X., Yu, L., Li, M., Song, P. (2020). Simulation of a supercritical CO_2 recompression cycle with zero emissions. Journal of Energy Engineering, 146(6):04020059.

[10] Chan, W., Lei, X., Chang, F., Li, H. (2020). Thermodynamic analysis and optimization of Allam cycle with a reheating configuration. Energy Conversion and Management, 224:113382.

[11] Dago, G. G. B., Frate, G. F., Baccioli, A., Ferrari, L., Alfarano, E., Colnago, A. (2025). Exergy analysis of the Allam cycle: Assessing the impact of regenerator performance on the cycle efficiency. Energy Conversion and Management, 345:120358.

[12] Avadhanula, V., Held, T, J. (2022). Integrated transient modeling of gas turbine and sCO_2 power cycle for exhaust heat recovery application. Proceedings of the 2022 sCO_2 Symposium. Echogen Power Systems.